



## LJMU Research Online

**Jasim, MH, Abdulridha, SQ, Beiram, AAH, Nasr, MS and Shubbar, A**

**Punching shear and load-deflection performance of RC flat slab made with hybrid concrete**

<http://researchonline.ljmu.ac.uk/id/eprint/25975/>

### Article

**Citation** (please note it is advisable to refer to the publisher's version if you intend to cite from this work)

**Jasim, MH, Abdulridha, SQ, Beiram, AAH, Nasr, MS and Shubbar, A (2025) Punching shear and load-deflection performance of RC flat slab made with hybrid concrete. *Advances in Science and Technology Research Journal*, 19 (5). pp. 156-172. ISSN 2080-4075 (Accepted)**

LJMU has developed [LJMU Research Online](#) for users to access the research output of the University more effectively. Copyright © and Moral Rights for the papers on this site are retained by the individual authors and/or other copyright owners. Users may download and/or print one copy of any article(s) in LJMU Research Online to facilitate their private study or for non-commercial research. You may not engage in further distribution of the material or use it for any profit-making activities or any commercial gain.

The version presented here may differ from the published version or from the version of the record. Please see the repository URL above for details on accessing the published version and note that access may require a subscription.

For more information please contact [researchonline@ljmu.ac.uk](mailto:researchonline@ljmu.ac.uk)

<http://researchonline.ljmu.ac.uk/>

# Punching shear and load-deflection performance of RC flat slab made with hybrid concrete

Mustafa Hamid Jasim<sup>1</sup>, Shereen Qasim Abdulridha<sup>2</sup>, Ammar A.H. Beiram<sup>1</sup>,  
Mohammed Salah Nasr<sup>2\*</sup> , Ali Shubbar<sup>3</sup>

<sup>1</sup> Al-Mussaib Technical Institute, Al-Furat Al-Awsat Technical University (ATU), 51009 Babylon, Iraq

<sup>2</sup> College of Engineering, University of Babylon, Iraq

<sup>3</sup> School of Civil Engineering and Built Environment, Liverpool John Moores University, Liverpool, UK

\* Corresponding author's e-mail: [eng511.mohammed.nasr@uobabylon.edu.iq](mailto:eng511.mohammed.nasr@uobabylon.edu.iq)

## ABSTRACT

Due to their various benefits, flat slabs are among the most commonly used flooring solutions worldwide. However, their use has been limited because of the risk of punching shear failure between the slab and the columns. Researchers have explored different solutions to address these issues, including using steel fiber-reinforced concrete (SFRC). Although this type of concrete offers advantages, its high cost can increase the overall expense of the structure compared to conventional concrete. An effective solution proposed was using hybrid concrete that combines SFRC in specific areas of the slab – namely, the center and around the columns – while utilizing conventional concrete for the remaining area. This study aims to investigate using hybrid concrete in flat slabs to enhance their punching shear resistance. The areas of fiber-reinforced concrete examined were circular shape. Limited research has explored the application of such hybrid concrete for shear strength, and even fewer studies have focused on the circular shapes of SFRC zones. Two parameters were considered in this study: (1) the radius of the hybrid concrete zone, which was set at two and three times the diameter of the column, and (2) the added percentage of steel fibers, specifically 0.5%, 1%, and 1.5%. Seven slabs were cast; one slab was made entirely of normal strength concrete (NSC) and served as a control, while six slabs were composed of hybrid concrete, a combination of NSC SFRC. The punching shear capacity, load-deformation behavior, crack patterns, failure mode, stiffness and ductility properties were investigated. The results indicated that hybrid concrete significantly enhanced punching shear resistance and other characteristics of flat slabs at both hybridization zones, specifically at two and three times the column radius. Additionally, the rate of improvement was directly proportional to the steel fiber content used. For example, with a fiber content of 1.5%, the punching shear capacity improved by 41.98% and 66.67% for the zones at two and three times the column radius, respectively. Furthermore, the uncracked stiffness increased by 30.9% and 44.6%, while the load capacity was enhanced by 42% and 66.7% for the same zones.

**Keywords:** flat slab, hybrid concrete, fiber reinforced concrete, punching shear, stiffness.

## INTRODUCTION

Flat slabs are among the most widely used flooring solutions globally, including in seismic regions [1]. Using flat reinforced concrete slabs for buildings offers several advantages compared to other reinforced concrete construction systems, such as drop-down slabs, column-headed slabs or beam-supported slabs. These benefits include creating more unobstructed space for a given floor height and decreasing the overall weight and

height of the structure [2]. However, the widespread application of flat slabs is limited by the potential for significant deformations and the risk of punching shear failure [3]. Shear failure caused by drilling occurs when a concrete slab fails directly beneath a concentrated load [4]. This type of failure happens when a concrete plug is pushed out of the slab. The displaced plug takes on the shape of a cone, with its upper area matching the area of the load [4]. The addition of fibers to cement-based composites enhances the matrix's

fracture energy by providing strength after cracks form [5–7]. This improvement increases ductility and helps control cracking and fatigue [6, 8, 9]. Additionally, depending on the type of fibers used, impact resistance can also be improved [10]. Using steel fibers to enhance the shear and cracking resistance of concrete column joints has proven to be effective. Additionally, steel fibers demonstrate significant effectiveness in structures subjected to lateral loads, such as during earthquakes, due to their capacity for energy absorption and dissipation [11]. Various methods, including fiber-reinforced polymers (FRPs), carbon fiber-reinforced polymers (CFRPs), external stirrups, shear stud, and steel fibers, are effective in strengthening defective reinforced concrete slabs against punching shear failure [12–14].

Shwalia et al. [15] conducted a study on the punching shear behavior of slab-to-column connections in flat slabs using mortar-infiltrated fiber concrete (MIFC). The fiber content used in the concrete was 6% by volume. They cast eight reinforced concrete slab specimens that had fixed dimensions and reinforcement, of which six were made with hybrid concrete (a mixture of normal strength concrete (NSC) and MIFC), while two served as control specimens made entirely of NSC. The MIFC was cast monolithically with NSC in a square-shaped area at a depth equivalent to 1.5 times the effective depth at the center of the slab. The study explored various parameters, including the location of the MIFC (at full thickness, in the top half, or in the bottom half of the slab) and the types of fibers used (hooked steel fiber and polypropylene fiber). A vertical load was applied upwards through a square column with dimensions of 100 mm. The results demonstrated that incorporating MIFC improved the punching shear strength in certain cases, depending on the fiber type and the location of the MIFC within the slab. The improvement in punching shear strength due to the use of MIFC ranged from 4% to 46% compared to the control slabs.

Zamri et al. [16] examined the punching shear behavior of flat slabs constructed with steel fibers and self-compacting concrete. They focused on various factors, including the types of shear reinforcement, the type of concrete used, the area of the steel fiber-reinforced self-compacting concrete around the column, and the thickness of the slab. The results indicated that flat slabs made with SFRSCC demonstrated effective crack control, good ductility, and strong punching shear

strength. Furthermore, the findings suggested that slabs with SFRSCC concentrated in a square area around the column can provide punching shear resistance comparable to that of slabs with SFRSCC applied across the entire surface. On the other hand, Salman and Hassan [17] conducted a study on the mechanical punching shear properties of steel fiber-reinforced concrete slabs. They cast two types of columns: rectangular and circular. Three different volume ratios of fibers were used in the study—0.5%, 1.0%, and 1.5%. The results showed that the mechanical properties improved with an increase in fiber content. Furthermore, it was observed that the square-sectioned slabs had a higher ultimate load capacity compared to the circular-sectioned slabs when the steel fiber dosage was 0.5% or 1.0%. However, at a steel fiber dosage of 1.5%, the ultimate load of the circular-sectioned slabs approached that of the square-sectioned slabs. Furthermore, Mu et al. [18] investigated how the orientation of steel fibers affects the punching shear behavior of round slabs. They also examined the influence of fiber volume fraction. Both a theoretical model and experimental methods were employed. The results indicated that the highest shear resistance was achieved with fibers oriented radially. Additionally, the ultimate shear resistance was improved by up to 24% at a 1% fiber volume fraction. Zhou et al. [19] investigated the use of ultra-high-performance fiber-reinforced concrete (UHPFRC) mixtures to enhance the punching shear capacity of slab-column connections. The composite slabs were constructed by casting UHPFRC in and around the center area of the column (square area), while the outer area of the slab was made with normal-strength concrete (NSC). The performance of these UHPFRC-based slabs was compared to that of the NSC slabs. The findings showed that the UHPFRC slabs resulted in a change in the mode of failure. Additionally, there were improvements in deformation capacity, punching shear strength, and initial stiffness when compared to the NSC slabs.

Moreover, Mahdi and Al-Tamimi [20] investigated the impact of buried pipelines on the punching shear capacity of seven lightweight concrete slabs. These slabs had fixed dimensions and varied distances between the pipelines and the loading area. They also examined the effect of reinforcing the area around the pipeline with high-strength concrete. The findings revealed that the punching shear capacity decreased as the pipeline moved closer to the loading area. Specifically,

there was a reduction of 28% when the pipeline was at 0 mm from the loading area and a 15% reduction at 50 mm, compared to the control sample. Conversely, using high-strength concrete increased the punching shear capacity by 25% and 10% for the same distances, respectively.

According to the literature, there are limited studies that have explored the punching shear behavior of hybrid concrete. Most research has focused on using a square area around the center column to apply conventional concrete, while very limited studies have examined circular shapes around the column with fiber-reinforced concrete using varying fiber content. Additionally, few studies have utilized micro-steel fibers to enhance the shear properties of concrete in hybrid concrete applications. Micro-steel fibers significantly contribute immediately after hairline cracks appear in the slab. Therefore, this study aims to investigate the resistance of reinforced concrete slabs to punching shear stress using a combination of conventional and fiber-reinforced concrete with different fiber fractions. Additionally, other properties such as load-deformation behavior, crack patterns, failure mode, stiffness and ductility were also analyzed.

## EXPERIMENTAL PROGRAM

### Materials

The following materials were used in the manufacturing of concrete specimens:

- Cement – locally produced limestone cement type CEM II/A-L-42.5 R was used. The cement properties were conformed to the Iraqi

specification No. 5 [21]. The chemical composition of cement is illustrated in Table 1.

- Fine aggregate – natural sand complying with the Iraqi specification No. 45 [22] was employed as fine aggregate. The grading of fine aggregate is shown in Figure 1.
- Coarse aggregate – locally available natural gravel with a maximum size of 14 mm was utilized as coarse aggregate. The grading of the aggregate, which was agreed with the Iraqi specification No. 45 [22], is presented in Figure 1.
- Steel fibers – micro steel fibers (type WSF0213, made in China) were used to reinforce the concrete specimens. The fibers length, diameter and aspect ratio were 13 mm, 0.2 mm and 65, respectively. Moreover, the tensile strength and modulus of elasticity of the fibers were 2300 MPa and 203 GPa, respectively.
- Water – tap water was utilized in casting and curing all the specimens.
- Steel reinforcement – deformed steel reinforcing bars of two different diameters (6 and 10 mm) were used. Table 2 summarizes the ultimate and yielding strength of the rebars.

**Table 1.** Chemical components of cement

Oxide composition	Content (%)	Limit of BS EN 197-1
(CaO)	61.21	----
SiO <sub>2</sub>	19.56	----
Al <sub>2</sub> O <sub>3</sub>	4.72	----
MgO	2.5	----
Fe <sub>2</sub> O <sub>3</sub>	5.51	----
SO <sub>3</sub>	1.87	≤ 3.5
Insoluble residue	0.97	----
Loss on ignition	1.73	----

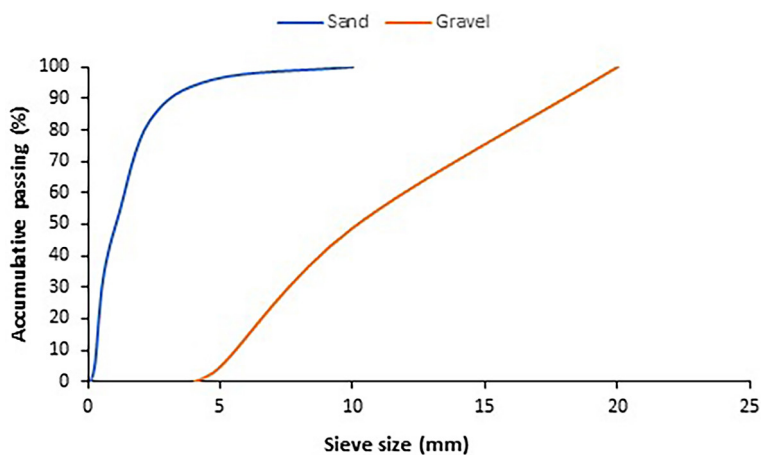


**Figure 1.** The grading of fine (sand) and coarse (gravel) aggregates

**Table 2.** Properties of the rebars

$\phi$ (mm)	Ultimate strength (Fu), MPa	Yielding strength (Fy), MPa
6	510	425
10	625	490

**Specimens’ preparation**

Seven square, flat slabs were cast with dimensions of  $900 \times 900 \text{ mm}^2$  and a thickness of 80 mm. Each slab had a circular column in the center, with dimensions of 100 mm diameter and 200 mm height. The slabs were designed to study the punching shear behavior, with adopting the maximum percentage of reinforcement ( $\rho_{max}$ ). The flexural reinforcing factor was installed according to ACI-318M-19 code, sections 8.6 and 8.7 [23], for each slab. The column was reinforced with 4  $\phi$  10 mm longitudinal reinforcement and 3 $\phi$ 6 mm shear reinforcement (stirrups) in accordance with ACI-318M-19 (sections 10.6 and 10.7 [23].

The concrete cover of slabs in all directions was 15 mm (according to ACI-318M-19, section 20.5.1 [23], and the effective depth was 65 mm. Figure 2 presents the details of reinforcement of the slab and column.

The study included replacing NSC with a specific diameter for the area surrounding the central column attached to the slab (instead of the entire area of the slab) with micro-steel fiber reinforced concrete to produce a hybrid concrete slab to study the extent of its effect on the slab behavior. Two parameters were considered: (1) the radius of the hybrid concrete zone and (2) the added percentage of steel fibers. One slab was made entirely of NSC, called a control slab. Six more slabs were cast and divided into two groups, each group consisting of three slabs. In the first group, the radius of the hybrid concrete zone was twice the radius of the column on which it was supported. In the second group, the radius of the hybrid concrete zone was three times the radius of the column. The slabs were reinforced with steel fibers for both groups of

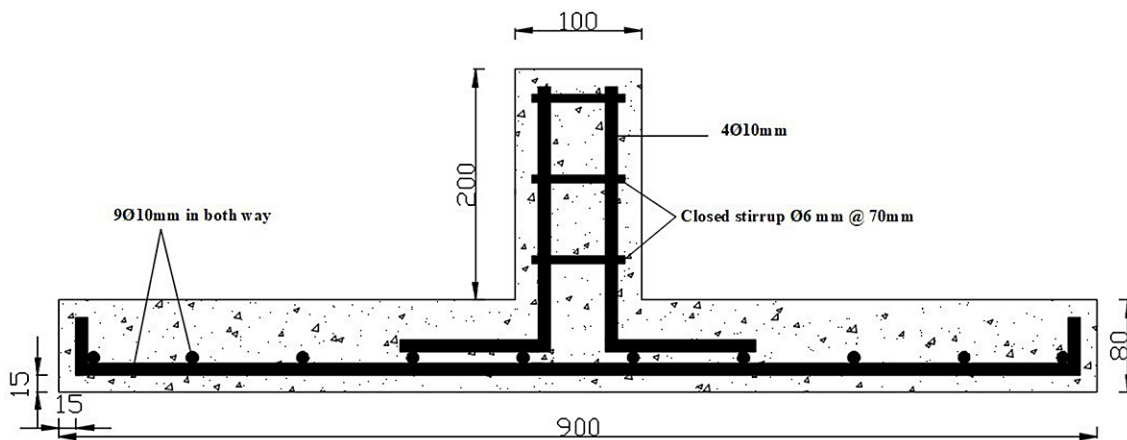


**Figure 2.** Details of steel reinforcement for a slab specimen

**Table 3.** Details of mix proportions

Mix designation	Group	Cement Kg/m <sup>3</sup>	Sand Kg/m <sup>3</sup>	Gravel Kg/m <sup>3</sup>	Water Kg/m <sup>3</sup>	Fiber, % (by vol.)
SNC	---	368	850	900	203	0
S2DF0.5	First*					0.5
S2DF1.0						1.0
S2DF1.5						1.5
S3DF0.5	Second**					0.5
S3DF1.0						1.0
S3DF1.5						1.5

\* The radius of SFC zone is two times of the column radius.

\*\* The radius of SFC zone is three times of the column radius.

0.5, 1, and 1.5% ratios. Table 3 shows the mix proportion details of the slabs.

### Specimen mixing and casting

Formwork was prepared from plywood with the necessary dimensions, and a preprepared reinforced steel mesh was placed. The mixing process for NSC and SFC was done using an electric horizontal mixer with a capacity of (0.09 m<sup>3</sup>). SFC and NSC were cast simultaneously in the hybrid specimens, as in Figure 3. As for the column, it was cast the day after the slab was cast using NSC.

### Test setup and procedure

After the end of the curing period (28 days), the reinforced samples were prepared by cleaning them and painting them white to facilitate observing the cracks during and after the test. A simple support was used for the slab, represented by a prepared steel frame, and it was placed in a testing device with a capacity of (600 kN). The loading protocol used to load the slabs was to transfer the axial load from the column to the slab. A cap cover was placed over the column to prevent local failure, and the load sensor, dial gauge, and bearing plates were placed between them, as shown in Figure 4.

## RESULTS AND DISCUSSION

### Estimating punching shear capacity

Table 4 presents the punching shear capacity recorded experimentally for the slab specimens adopted in the present study. Adding micro-steel fibers with ratios 0.5%, 1% and 1.5% respectively to the specimens with a radius of the hybrid concrete zone twice the radius of the column increases the punching capacity by about 15.56%, 24.69% and 41.98%. Also, for specimens having (a radius of a hybrid concrete zone three times the radius of the column), the increasing percentages of punching shear were 28.40%, 48.15% and 66.67% respectively. It can be summarized that adding micro-steel fiber to the hybrid slab (the radius of a hybrid concrete zone was two or three times the radius of the column) with ratios 0.5%, 1% and 1.5% contributes to increase the punching shear capacity of percentages between 15.56% to 66.67%. The bridging action of micro-steel fibers added to the specimen could be responsible for this behavior and improving the punching shear capacity, as many studies mentioned in this field like [24–27]. The theoretical value of the punching shear for the slab specimens under consideration



Figure 3. Specimen preparation and casting



Figure 4. Test setup of slab specimen

there were three equations presented in ACI 318-19 [23] listed below (1, 2, and 3):

$$V_c = 0.33 \cdot \lambda_s \lambda \cdot \sqrt{f_c} \cdot b_o \cdot d \quad (1)$$

$$V_c = \left(0.17 + \frac{0.33}{\beta}\right) \lambda_s \cdot \lambda \cdot \sqrt{f_c} \cdot b_o \cdot d \quad (2)$$

$$V_c = \left(0.17 + \frac{0.083 \alpha_s \cdot d}{b_o}\right) \cdot \lambda_s \lambda \cdot \sqrt{f_c} \cdot b_o \cdot d \quad (3)$$

where:  $\beta$  – the ratio between length to width of the column (for circular column  $\beta = 1$ ),  $\lambda = 1$  (for normal concrete),  $\lambda_s = \sqrt{\frac{2}{1 + 0.004 d}} \leq 1$ ,  $f_c$  – compressive strength (for cylinder, MPa),  $b_o$  – critical punching perimeter at a distance of  $d/2$  from the column face (mm),  $d$  – the effective depth (mm),  $\alpha_s = 40$  for (interior column).

Table 4. Punching shear capacity of slab specimen (ACI 318-19 and experimentally)

Specimen	Vexp. kN	%Vexp. increase	fc cylinder MPa	Vtheo (kN)	Vexp/Vtheo.-1a	Vtheo. kN	Vexp/Vtheo.-1b	Vtheo (kN)	Vexp/Vtheo.-1c
				ACI-318-1a		ACI 318-1b		ACI-318 1c	
SNC	81.0	----	18.05	42.23	1.918	71.53	1.132	71.10	1.139
S2DF0.5	93.6	15.56	20.58	45.10	2.076	76.39	1.225	75.93	1.233
S2DF1.0	101	24.69	22.14	46.78	2.159	79.24	1.275	78.76	1.282
S2DF1.5	115	41.98	23.34	48.03	2.395	81.36	1.414	80.86	1.422
S3DF0.5	104	28.40	20.58	45.10	2.306	76.39	1.361	75.93	1.370
S3DF1.0	120	48.15	22.14	46.78	2.565	79.24	1.514	78.76	1.524
S3DF1.5	135	66.67	23.34	48.03	2.811	81.36	1.659	80.86	1.670
Average					2.319		1.369		1.377

These three values of punching capacity were calculated for every slab specimen, track Table 9. The values of punching shear estimated by Equations 2 and 3 were so close to each other and conservative to some extent compared to values of punching shear obtained experimentally for normal concrete slab (SNC specimen) and hybrid slab specimens having different ratios of micro-steel fibers, whereas results of Equation 1 were underestimated and may be considered so conservative, as shown in Figure 5. Pani L and Stochino F 2020 [28] referred to the validity of Equation 2 for the square column case (the area of subjecting loads on the slab was square), although this study depends on the equation presented by ACI 318-11 and the existing of some difference between these two equations. From the experimental results of punching shear for hybrid slab specimens having different ratios of micro-steel fiber and comparing with ACI 318-19 equations, Equation 2 was the most recommended to be used.

### Developing crack patterns and failure modes

In the early stages of loading, no cracks appeared in the tested slab specimens until reaching a load amount that caused the first crack ( $F_{cr}$ ), which was recorded for all specimens in Table 5. Cracks began to appear with increasing load amounts applied to the specimens. First cracks were observed to appear approximately at a distance equal to  $d/2$  (half the column diameter) diagonally from the face of the column, and then circumferential cracks appeared. In the first specimen having no fibers (SNC) the diagonal and circumferential cracks appeared and grew rapidly with spalling and crushing of the concrete cover in addition to the punching failure existence as shown in the Figure 6 below. All slab specimens with hybrid concrete adopted in the present study overcame the punching failure although part of the concrete cover was damaged in some specimens. It is worth knowing that the damage that

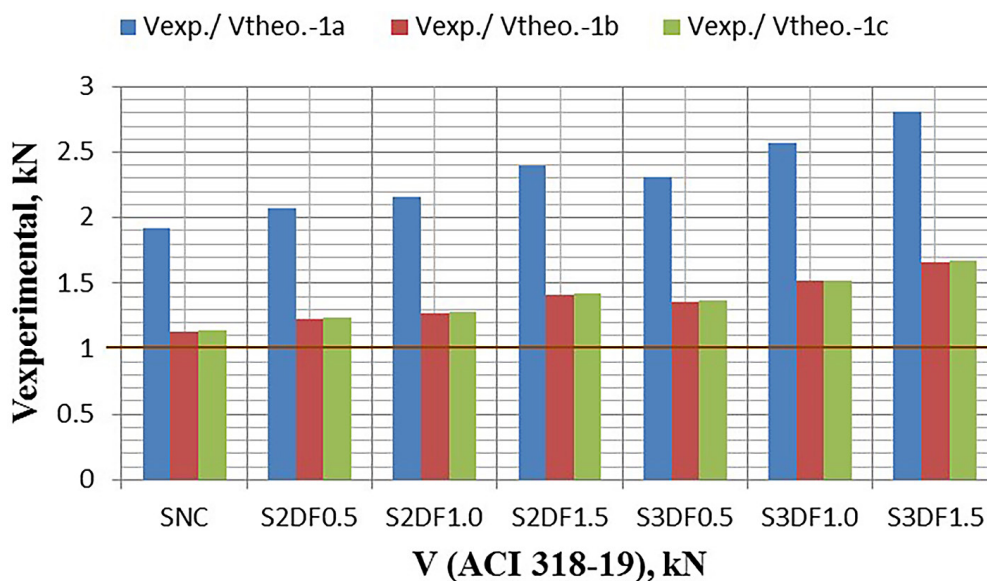


Figure 5. Ratios of punching shear of slab specimens by ACI 318-19 and experimentally

Table 5. First crack load of slab specimens

Slab specimen	F <sub>cr</sub> , kN	F <sub>cr</sub> , %	F <sub>ult</sub> , kN	F <sub>ult</sub> , %
SNC	23	--	81	--
S2DF0.5	27.6	20.0	93.6	15.6
S2DF1.0	31.5	37.0	101	24.7
S2DF1.5	35.2	53.0	115	42.0
S3DF0.5	28.1	22.2	104	28.4
S3DF1.0	32	39.1	120	48.1
S3DF1.5	37.1	61.3	135	66.7

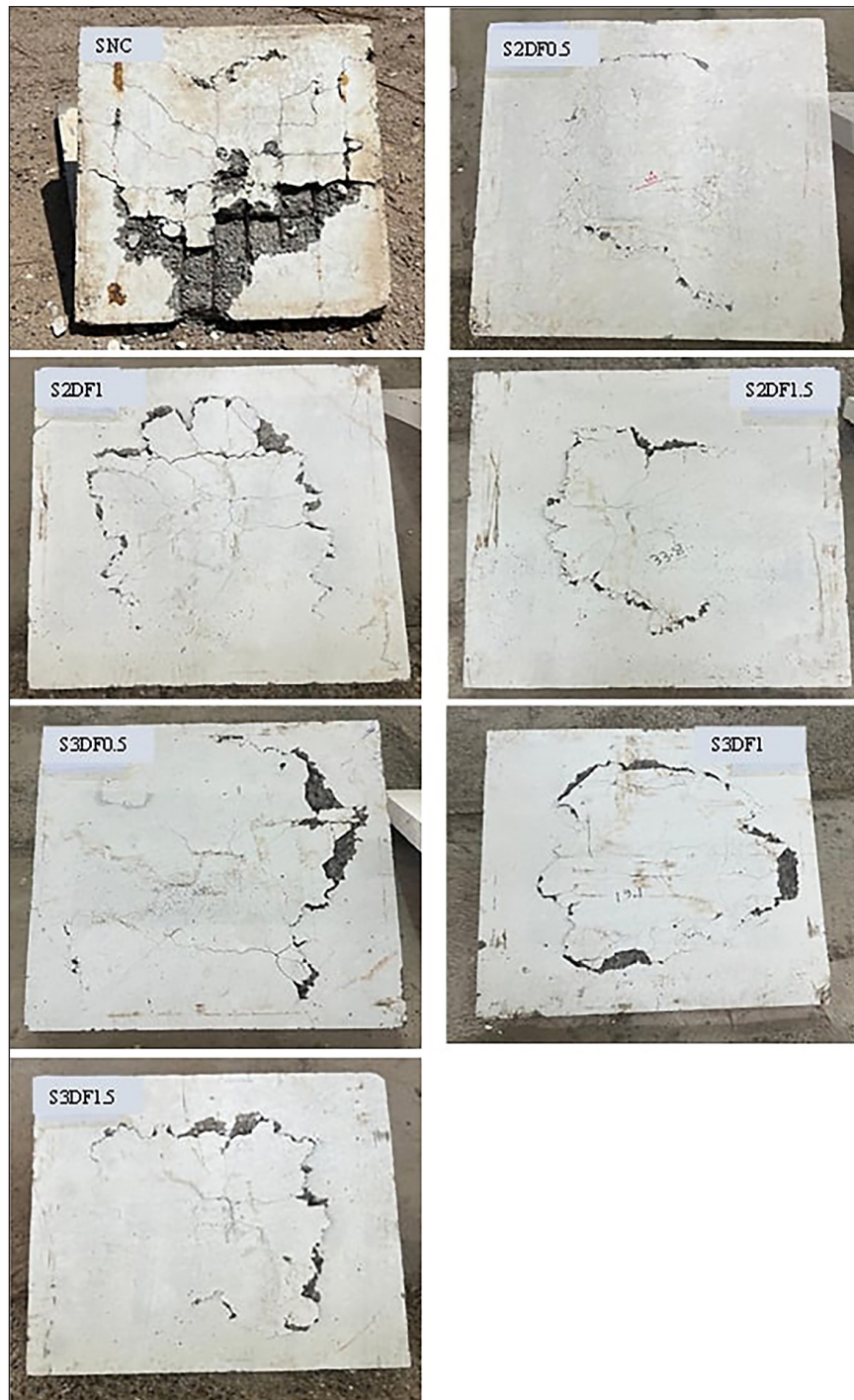


Figure 6. Crack patterns of slabs specimens

exists in part of the concrete cover in specimens with micro-steel fibers happened at the latest stages of loading and could be considered logically and justified where it occurred when the ultimate load capacity increased ( $F_{ult}$ ) by about 15.6% to 66.7%. The addition of micro-steel fibers to the concrete slab specimens significantly delayed the appearance of the first cracks. The bridging action of these fibers in the cracked regions plays

a crucial role in this process, a phenomenon also observed in a prior study by Roesler et al. [29], which investigated the inclusion of synthetic fibers in concrete slabs. This behavior demonstrates the effectiveness of micro-steel fibers in hybrid concrete slab specimens in preventing and delaying crack formation, which aligns with previous studies done on different types of fibers used to enhance the concrete slab [14, 30].

The percentage of increase in the load causing the onset of cracking for the three specimens with a diameter of hybrid concrete twice the diameter of the concrete column was about 20%, 37%, and 53%, respectively, while for the other three specimens with a diameter of hybrid concrete three times the diameter of the concrete column, it was about 22.2%, 39.1%, and 61.3%, respectively, see Figure 7. The present results are so close to that observed by Shi et al [31], where an improvement in the cracking strength of slab specimens with steel fibers by about 47% compared with the adopted plain concrete slab. It was noted that the percentages of increase in the amount of load causing the onset of cracking for the specimens containing the same percentage of micro-steel fibers and a different diameter of hybrid concrete were somewhat close. That is, the effect of increasing the diameter of hybrid

concrete was not clear on the load causing the onset of cracking. This may be attributed to the fact that the difference between the diameters of the hybrid concrete in the two adopted cases was not large enough to show the improvement in the amount of load causing the first cracking clearly.

### Load-deflection response

Figure 8 introduces the load-deflection behavior of flat slab specimens, normal and hybrid with different areas of hybrid concrete and different ratios of micro-steel fiber. In general, it was noted that the non-hybrid and non-fiber (SNC) model fails earlier compared to the hybrid and fiber-containing specimens, in terms of the maximum load and maximum deflection.

The load capacity of slab specimens ( $F_{ult}$ ) increases as the ratio of micro-steel fiber increases

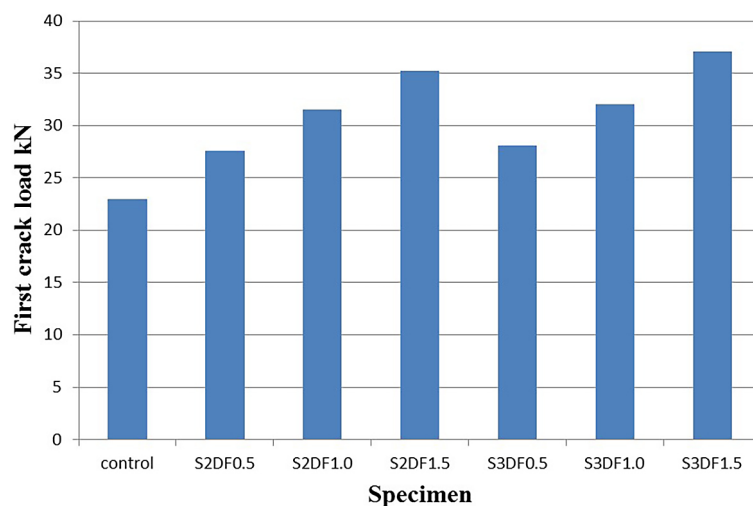


Figure 7. First crack loads of slab specimens

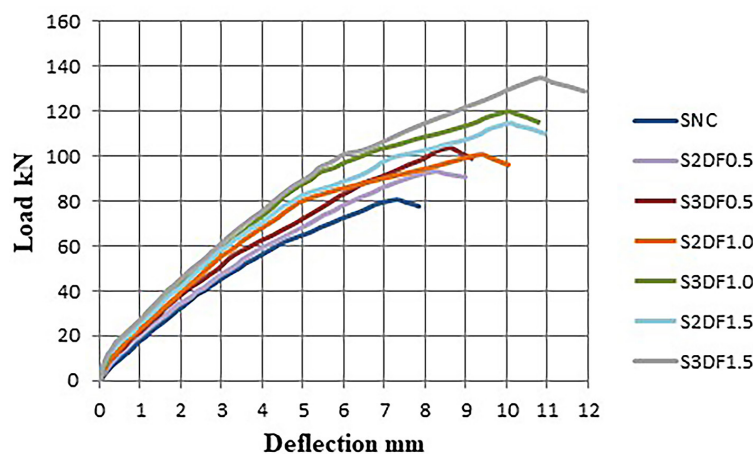


Figure 8. Load-deflection of all flat slab specimens

when the radius of the hybrid concrete zone was twice the radius of the column, about 15.6%, 24.7%, 42.0%. When the radius of the hybrid concrete zone was three times the radius of the column the increasing percentages were 28.4%, 48.1%, 66.7%. That is, the increase in the ultimate load mostly rises by 1.5 to 2 times when fibers ratio was increased from 0.5% to 1% and 1.5% in both cases (the radius of the hybrid concrete double and three times the column radius), see Table 6. Zazue et al. [32] reported a significant enhancement in the ultimate load capacity of slab specimens with the incorporation of steel-polypropylene fiber ratios ranging from 0% to 1.8%, achieving an increase of approximately 33.96% to 52.19%. These findings align well with the results obtained in the present study. Also, the study by Yu et al. [33] showed the enhancement of deformability

and load capacity of slabs that have steel fibers. On the other hand, the ultimate deflection ( $D_{ult.}$ ) also improved, increasing by 13.7%, 28.8% and 38.4% when the radius of the hybrid concrete was double the column radius with ratios of steel fiber 0.5%, 1%, and 1.5% respectively. Increasing the radius of hybrid concrete to three times the concrete column leads to an increase in the ultimate deflection that occurred in the slab specimens adopted by 17.8%, 37.0% and 47.9% for the same nominated ratios of the steel fibers respectively, track Figures 9 to 13.

For the purpose of studying the cases more accurately, specimens with same area (or radius) of fiber-reinforced concrete but with different percentages of fibers were presented in addition to the reference model in Figures 12 and 13. Also, specimens containing the same ratio of fibers were presented

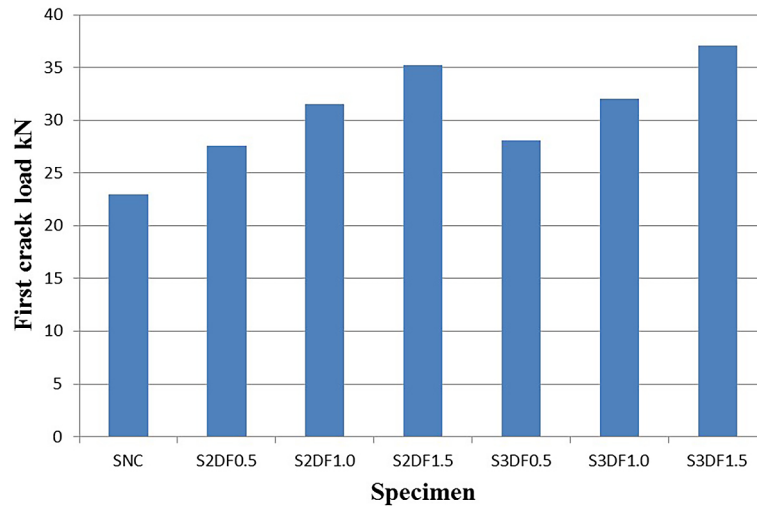


Figure 9. The effect of micro steel fiber on ( $F_{cr}$ ) of slab specimens

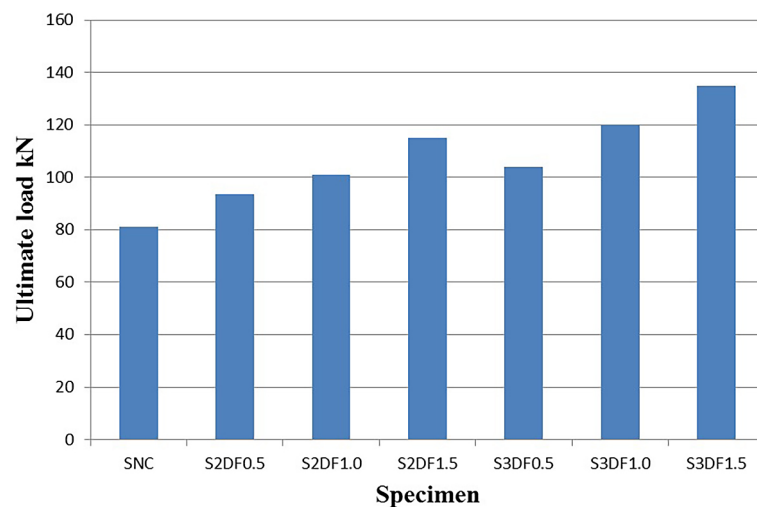


Figure 10. The effect of micro steel fiber on ( $F_{ult}$ ) of slab specimens

in addition to the reference model (SNC) in Figure 14. That is, when the radius of the hybrid concrete increases to three times the concrete column and the percentage of steel fibers remains constant at 0.5%, the maximum load increases by 11.1%, and increases by 18.8% and 17.4%, respectively, at a fiber percentage of 1.0% and 1.5% respectively. At the same time when the radius of hybrid concrete has increased from double to triple and at the same steel fiber ratio, the maximum deflection increases by 3.6%, 6.4%, and 6.9% respectively.

**Stiffness**

Stiffness degradation of a structural element is an essential indication that could reflect its accumulated deterioration, where it could give an acceptable indication that reflects the ductility,

residual capacity, and, thus, the members’ safety [34–36]. Table 7 shows the two parameter values of the stiffness calculated for the adopted slab specimens. Where  $K_i$  is the uncracked stiffness and can be found by dividing the value of load to displacement at the first cracking load. The second parameter  $K_u$  can be calculated by dividing the load by displacement at the ultimate state of each slab specimen. So the stiffness degradation ( $St.D$ ) could be found which is the ratio between the two parameters ( $K_u/K_i$ ), track Table 7. The uncracked stiffness ( $K_i$ ) of slab specimens when the radius of the hybrid concrete was double the column radius having ratios of steel fiber 0.5%, 1%, and 1.5%, respectively, have increased by about 7.6%, 18.7%, 30.9%, in comparison with the slab specimen without SNC. On the other hand, for slab specimens with radius of hybrid

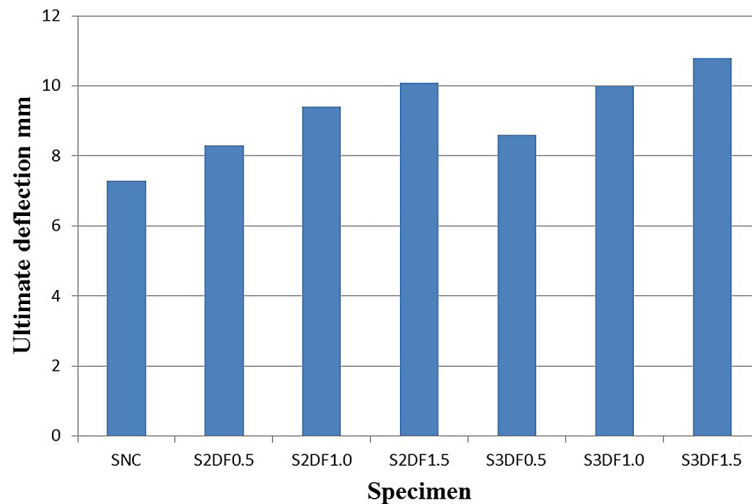


Figure 11. The effect of micro steel fiber on ( $D_{ult}$ ) of slab specimens

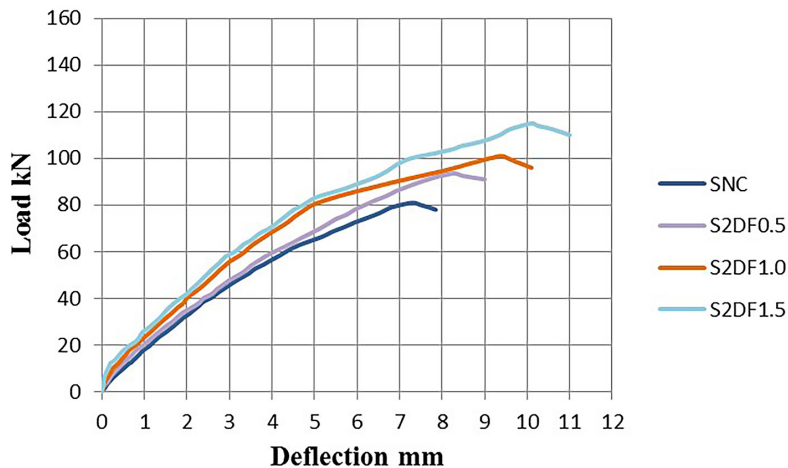


Figure 12. The effect of micro-steel fiber ratio on load deflection behavior for specimens with hybrid diameter twice the column

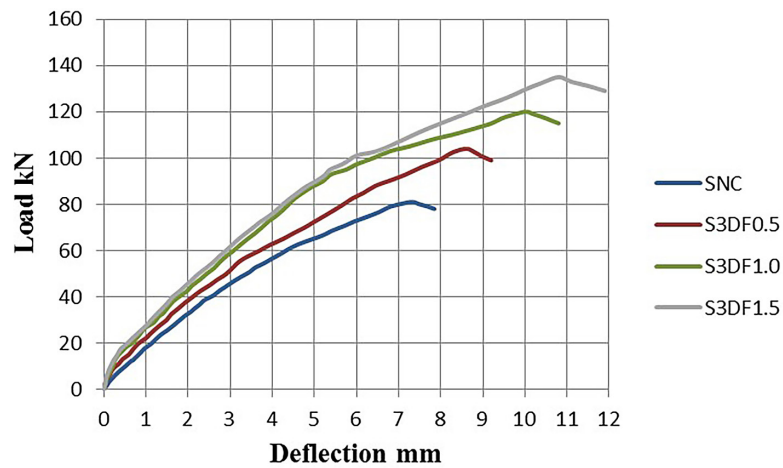


Figure 13. The effect of micro-steel fiber ratio on load deflection behavior for specimens with hybrid diameter three times the column

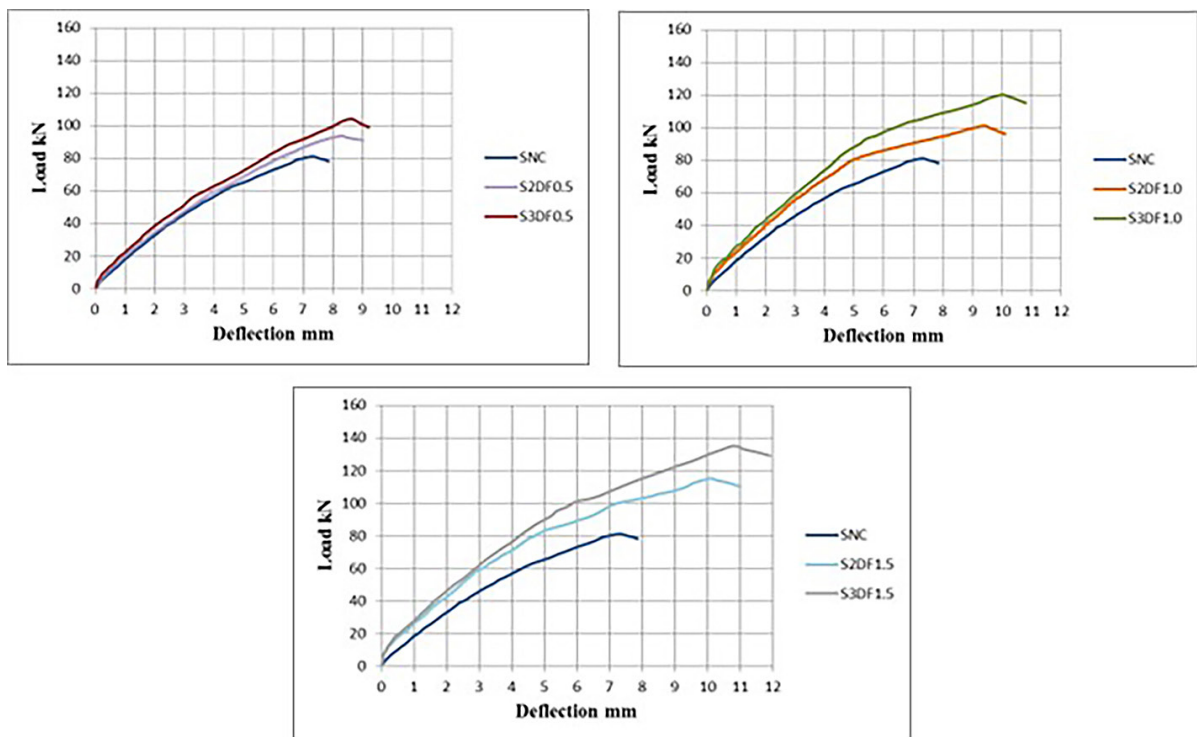


Figure 14. The effect of hybrid concrete diameter (twice and three times the concrete column) on load deflection behavior

Table 6. The ultimate deflection of slab specimens

Specimen	$F_{ult}$ (kN)	$D_{ult}$ (mm)	% D ult.
SNC	81	7.3	0.0
S2DF0.5	93.6	8.3	13.7
S2DF1.0	101	9.4	28.8
S2DF1.5	115	10.1	38.4
S3DF0.5	104	8.6	17.8
S3DF1.0	120	10	37.0
S3DF1.5	135	10.8	47.9

**Table 7.** Parameters of stiffness degradation and its calculations for slab specimens

Sample	Load (kN)	$D_{ult}$ (mm)	$K_u$	$F_{cr}$ (kN)	Def. at crack (mm)	$K_i$	% $K_i$	$St_D$	% $St_D$ decreased
SNC	81	7.3	11.10	23	1.3	17.69	----	0.63	----
S2DF0.5	93.6	8.3	11.28	27.6	1.45	19.03	7.6	0.59	5.5
S2DF1.0	101	9.4	10.74	31.5	1.5	21.00	18.7	0.51	18.4
S2DF1.5	115	10.1	11.39	35.2	1.52	23.16	30.9	0.49	21.6
S3DF0.5	104	8.6	12.09	28.1	1.35	20.81	17.6	0.58	7.4
S3DF1.0	120	10	12.00	32	1.35	23.70	34.0	0.51	19.3
S3DF1.5	135	10.8	12.50	37.1	1.45	25.59	44.6	0.49	22.1

concrete three times the concrete column, the uncracked stiffness also increased by about 17.6%, 34.0%, and 44.6%. It can be noticed clearly the effect of increasing the radius of hybrid concrete from double to triple the concrete column for the same percentage of micro-steel fiber, where  $K_i$  increased from 7.6% to 17.6%, 18.7% to 34.0%,

and also from 30.9% to 44.6%. Also, the stiffness degradation of slab specimens S2DF0.5, S2DF1.0, and S2DF1.5 was reduced by 5.5%, 18.4%, and 21.6%, and 7.4%, 19.3%, and 22.1% for specimens S3DF0.5, S3DF1.0, and S3DF1.5, respectively compared with the specimen without SNC, see Figures 15 and 16. These results

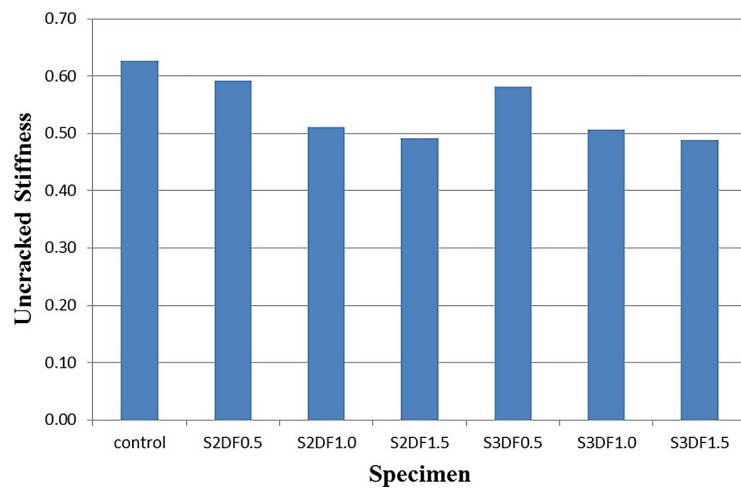


**Figure 15.** Uncracked stiffness of slab specimens

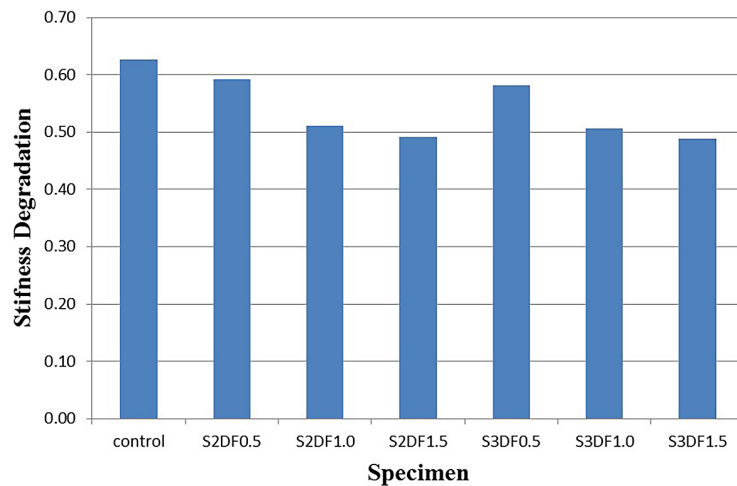


**Figure 16.** Stiffness degradation of slab specimens

showed the ability of micro-steel fiber to increase the stiffness of slab specimens and presented that using hybrid concrete with micro-steel fiber with a radius of double or triple the radius of the concrete column improves the stiffness compared with no fiber slab specimen. This enhancement in the behavior when adding micro-steel fiber to the slab specimens can be attributed to cracking load and accompanied deflection that rather increased. The present result agreed with a previous study of Labib [26] which showed enhancement in the behavior of concrete slab specimens when adding steel-polypropylene fibers. Also, Yehia et al 2023 [37] stated increasing ductility when adding micro steel fiber to the slab specimens.

### Ductility

Observation of the ductility of the slab specimens adopted could reflect their ability to deflect at or close to the failure load, that is, in the elastic domain, without loss in strength [38, 39]. In

general, the ductility index was calculated from a load-deflection diagram. It could be calculated based on either the ultimate stage ( $D_{lu}=D_u/D_y$ ) or the peak stage ( $D_{lp}=D_p/D_y$ ). Previous studies [40–42] found no obvious trend in the ductility of a concrete member with fiber depending on the peak, whereas the ultimate one ( $D_{lu}$ ) is methodical with an evident trend in the behavior. Thus, the ultimate ductility indices were depended on in the present study. The parameters needed to calculate  $D_{lu}$  were deflection at the ultimate stage which can be easily specified from the load-deflection curve, and deflection at yield which needs some technique because the yield of the concrete member was not clear, so a method recommended by many researchers [5, 43] summarized as draw the line of  $P_u$ , draw the line of  $0.75 P_u$ , draw a line passing through  $0.75 P_u$  line until line of  $P_u$ , after that drawing a perpendicular line to the horizontal axis where the point specified is  $D_y$ , as shown in Figure 17. Table 8 shows the parameters and  $D_{lu}$ 's increasing percentages for slab specimens under

**Table 8.** Ductility of slab specimens

Specimen	$F_{ult}$ (kN)	$0.75\% F_{ult}$ (kN)	$D_{ult}$	$D_y$	$D_{lu}$	% $D_{lu}$
SNC	81	60.75	7.3	6.08	1.20	----
S2DF0.5	93.6	70.20	8.3	6.70	1.24	3.20
S2DF1.0	101	75.75	9.4	6.08	1.55	28.8
S2DF1.5	115	86.25	10.1	7.24	1.40	16.2
S3DF0.5	104	78.00	8.6	7.05	1.22	1.60
S3DF1.0	120	90.00	10	6.65	1.50	25.2
S3DF1.5	135	101.25	10.8	7.80	1.38	15.3

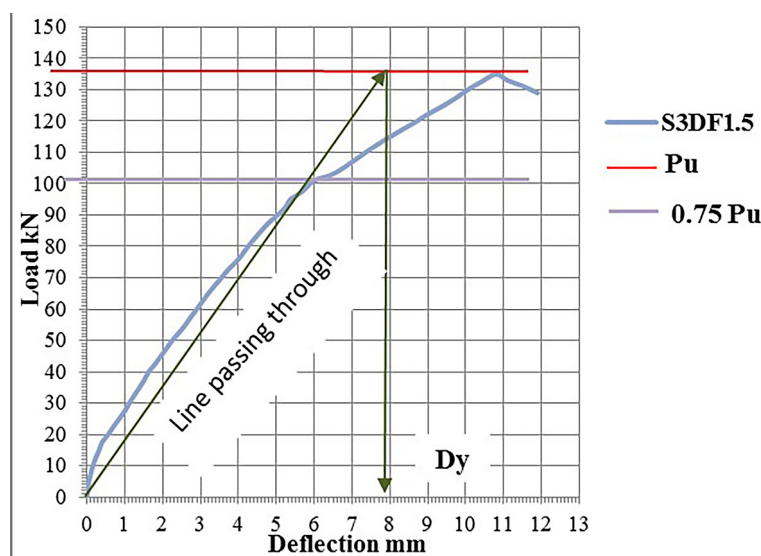


**Figure 17.** Specifying  $D_y$  for S3DF1.5

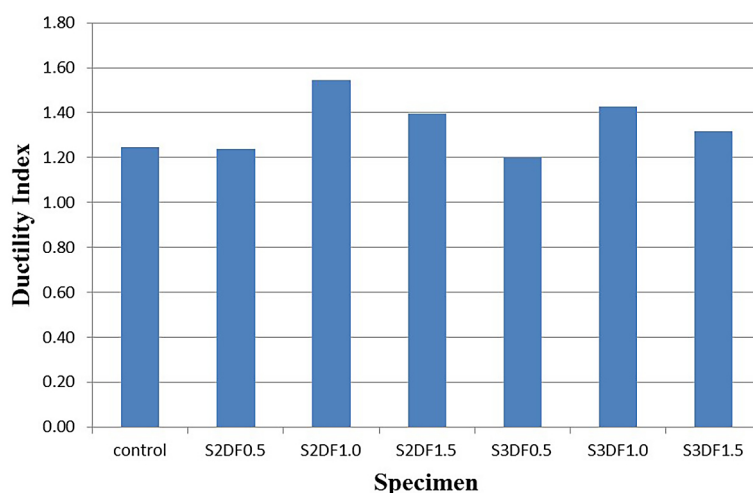


Figure 18. The effect of DI<sub>u</sub> on the slab with micro steel fiber

consideration. When micro-steel fiber was added to the slab specimens, it could be noticed the ductility indices were increased, this supports the idea of increasing the ability of these slab specimens to absorb energy and agrees with previous studies done on different structural members having fibers like [5, 44–47]. Although the percentages of increase were disparate, the maximum increase of  $D_{iu}$  was in specimens with 1% micro-steel fibers which were 28.8% and 25.2% for specimens S2DF1.0 and S3DF1.0, respectively (Figure 18).

## CONCLUSIONS

Based on the experimental work conducted and the results obtained, the following conclusions are extracted:

The punching capacity was enhanced with the addition of micro-steel fibers. When the radius of the hybrid concrete zone was twice that of the column, the punching capacity increased by 15.56%, 41.98%, and 48.15% at fiber ratios of 0.5%, 1%, and 1.5%, respectively. When the radius was three times that of the column, the improvements were 24.69%, 28.40%, and 66.67% for the same fiber contents.

Based on experimental punching shear results for hybrid slab specimens with varying micro-steel fiber ratios, Equation 1.b from ACI 318-19 was recommended. When the radius of the hybrid concrete increased from two to three times the radius of the concrete column, the maximum load improved by 11.1%, 18.8% and 17.4%, respectively, at fiber levels of 0.5, 1.0 and 1.5%. Increasing the radius of hybrid concrete from double to triple the

size of the concrete column while maintaining the same percentage of micro-steel fiber results in a noticeable increase in uncracked stiffness. Specifically, the uncracked stiffness ( $K_u$ ) increased as follows: for micro-steel fiber ratios of 0.5%, it rose from 7.6% to 17.6%; for 1.0%, from 18.7% to 34.0%; and for 1.5%, from 30.9% to 44.6%.

The combination of hybrid concrete (NSC and SFRC) improved the ductility indices, resulting in enhanced energy absorption capacity of the slab specimens. Although the increase percentages vary, the  $D_{iu}$  in specimens with 1% micro-steel fibers improved by 28.8% for S2DF1.0 and 25.2% for S3DF1.0.

The addition of micro-steel fibers to the concrete slab specimens significantly postponed the appearance of the first cracks. The percentage increases in the load required to initiate cracking for the specimens with a diameter of hybrid concrete twice and three times that of the concrete column were (20%, 37%, and 53%), and (22.2%, 39.1%, and 61.3%), respectively.

The present study has conducted several tests to investigate the behavior of flat slabs subjected to punching shear; however, it has several limitations. One significant limitation is that the study did not include a theoretical analysis using specialized software such as Abaqus and ANSYS, in addition to the experimental component. Furthermore, the study did not explore the behavior of hybrid concrete slabs under seismic or dynamic loads. Additionally, the parameters examined in this research were somewhat limited; for example, the effects of varying the slab thickness or changing the type of fibers were not considered.

Therefore, the authors recommend that future research be more comprehensive to address these limitations. Specifically, it is advisable to investigate the impact of using hybrid steel fibers, including both macro and micro steel fibers. The authors also suggest the development of hybrid concrete that combines conventional concrete with ultra-high-performance concrete, as the latter possesses unique properties. Utilizing ultra-high-performance concrete could potentially reduce the diameter of the hybrid concrete, resulting in lower construction costs.

## REFERENCES

1. Coronelli D., Lamperti Tornaghi M., Martinelli L., et al. Testing of a full-scale flat slab building for gravity and lateral loads. *Eng. Struct.* 2021; 243: 112551. <https://doi.org/10.1016/j.engstruct.2021.112551>
2. Torabian A., Isufi B., Mostofinejad D., Ramos A.P. Behavior of thin lightly reinforced flat slabs under concentric loading. *Eng. Struct.* 2019; 196: 109327. <https://doi.org/10.1016/j.engstruct.2019.109327>
3. Bursać S., Bešević M., Vojnić Purčar M., Kozarić L., Đurić N. Experimental analysis of punching shear strength of eccentrically loaded slab with the opening along the face of the internal column. *Eng. Struct.* 2021; 249: 113359. <https://doi.org/10.1016/j.engstruct.2021.113359>
4. Talib H.Y., Al-Salim N.H.A. Improving punching shear in flat slab by replacing punching shear reinforcement by ultrahigh performance concrete. *Int. J. Eng.* 2022; 35(8): 1619–1628.
5. Abdulridha S.Q., Nasr M.S., Al-Abbas B.H., Hasan Z.A. Mechanical and structural properties of waste rope fibers-based concrete: An experimental study. *Case Stud. Constr. Mater.* 2022; 16: e00964.
6. Jasim M.H., Nasr M.S., Beiram A.A.H., Heil S.M. Mechanical, durability and electrical properties of steel fibers reinforced concrete. *Adv. Sci. Technol. Res. J.* 2024; 18(7): 163–175.
7. Hasan Z.A., Jasim M.H., Shaker A.A., Nasr M.S., Abdulridha S.Q., Hashim T.M. Experimental investigation on using electrical cable waste as fine aggregate and reinforcing fiber in sustainable mortar. In: *Annales de Chimie Science des Matériaux*, 2023; 47.
8. Jasim M.H., Al-Salim N.H.A. Enhancement Behavior of Reinforced Concrete Beam with Transverse Holes Under Combined Twisting and Bending Using Steel Fiber. In: *Journal of Physics: Conference Series*, vol 1973. IOP Publishing; 2021: 12027.
9. Khan M., Cao M., Xie C., Ali M. Effectiveness of hybrid steel-basalt fiber reinforced concrete under compression. *Case Stud. Constr. Mater.* 2022; 16: e00941.
10. Aidarov S., Mena F., de la Fuente A. Structural response of a fibre reinforced concrete pile-supported flat slab: full-scale test. *Eng. Struct.* 2021; 239: 112292. <https://doi.org/10.1016/j.engstruct.2021.112292>
11. Nguyen-Minh L., Rovňák M., Tran-Quoc T., Nguyenkim K. Punching shear resistance of steel fiber reinforced concrete flat slabs. *Procedia Eng.* 2011; 14: 1830–1837. <https://doi.org/10.1016/j.proeng.2011.07.230>
12. Said M., Adam M.A., Arafa A.E., Moatasem A. Improvement of punching shear strength of reinforced lightweight concrete flat slab using different strengthening techniques. *J. Build. Eng.* 2020; 32: 101749. <https://doi.org/10.1016/j.jobbe.2020.101749>
13. Ghayeb H.H., Atea R.S., Al-Kannoon M.A.-A., Lee F.W., Wong L.S., Mo K.H. Performance of reinforced concrete flat slab strengthened with CFRP for punching shear. *Case Stud. Constr. Mater.* 2023; 18: e01801. <https://doi.org/10.1016/j.cscm.2022.e01801>
14. Bassurucu M., Turk K., Turgut P. The effect of hybrid fiber and shear stud on the punching performance of flat-slab systems. *J. Build. Eng.* 2023; 77: 107555.
15. Shwalia A.S.I., Al-Salim N.H.A., Al-Baghdadi H.M. Enhancement punching shear in flat slab using mortar infiltrated fiber concrete. *Civ. Eng. J.* 2020; 6(8): 1457–1469. <https://doi.org/10.28991/cej-2020-03091560>
16. Zamri N.F., Mohamed R.N., Awalluddin D., Abdullah R. Experimental evaluation on punching shear resistance of steel fibre reinforced self-compacting concrete flat slabs. *J. Build. Eng.* 2022; 52: 104441. <https://doi.org/10.1016/j.jobbe.2022.104441>
17. Hassan R.F. Experimental investigation on the impact of micro-steel fibers on the flat slabs' punching shear resistance. *Tikrit J. Eng. Sci.* 2023; 30(3): 71–80.
18. Mu R., Mei S., Chen J., et al. Effect of steel fiber orientation on punching shear resistance of steel fiber reinforced cementitious composites round slabs. *J. Build. Eng.* 2024; 89: 109289. <https://doi.org/10.1016/j.jobbe.2024.109289>
19. Zhou Y., Shou H., Li C., Jiang Y., Tian X. Punching shear behavior of ultra-high-performance fiber-reinforced concrete and normal strength concrete composite flat slabs. *Eng. Struct.* 2025; 322: 119123. <https://doi.org/10.1016/j.engstruct.2024.119123>
20. Mehdi W.S., Al-Tameemi H.A. Punching shear capacity of lightweight concrete flat slabs with embedded pipelines. In: *AIP Conference Proceedings*, 2024; 3249.
21. Iraqi Standard NO.5. Portland Cement. Central Organization for Standardization and Quality Control, Baghdad, Iraq; 2019.
22. Iraqi Standard NO.45. Aggregate from Natural Sources for Concrete and Building Construction.

- Central Organization for Standardization and Quality Control, Baghdad, Iraq; 2010.
23. Institute) A.C.I. (American C. ACI 318-19: Building code requirements for structural concrete. 2019.
  24. Mohammed A.H., Mubarak H.M., Hussein A.K., Abulghafour T.Z., Nassani D.E. Punching shear characterization of steel fiber-reinforced concrete flat slabs. *HighTech Innov. J.* 2022; 3(4): 483–490.
  25. Kim D.J., Park S.H., Ryu G.S., Koh K.T. Comparative flexural behavior of hybrid ultra high performance fiber reinforced concrete with different macro fibers. *Constr. Build. Mater.* 2011; 25(11): 4144–4155.
  26. Labib W.A. Evaluation of hybrid fibre-reinforced concrete slabs in terms of punching shear. *Constr. Build. Mater.* 2020; 260: 119763.
  27. Abdel-Rahman A.M., Hassan N.Z., Soliman A.M. Punching shear behavior of reinforced concrete slabs using steel fibers in the mix. *HBRC J.* 2018; 14(3): 272–281.
  28. Pani L., Stochino F. Punching of reinforced concrete slab without shear reinforcement: Standard models and new proposal. *Front. Struct. Civ. Eng.* 2020; 14: 1196–1214.
  29. Roesler J.R., Altoubat S.A., Lange D.A., Rieder K.-A., Ulreich G.R. Effect of synthetic fibers on structural behavior of concrete slabs-on-ground. *ACI Mater. J.* 2006; 103(1): 3.
  30. Zainal S.M.I.S., Hejazi F., Mafaileh A.M.A. Strengthening of Reinforced Concrete slabs using macro and micro synthetic fibers. In: *Structures*, vol 51. Elsevier; 2023: 1579–1590.
  31. Shi F., Pham T.M., Tuladhar R., Deng Z., Yin S., Hao H. Comparative performance analysis of ground slabs and beams reinforced with macro polypropylene fibre, steel fibre, and steel mesh. In: *Structures*, vol 56. Elsevier; 2023: 104920.
  32. Zaezue S.J., Hadi W.K. Effect of hybrid steel-polypropylene fiber on punching shear behavior of flat slab with an opening. *Przegląd Nauk. Inżynieria i Kształtowanie Środowiska* 2023; 32.
  33. Yu J., Sneed L.H., Zhai T., Li Y. Study of the shear bond behavior of a hybrid fiber-reinforced concrete (HyFRC) composite slab. *Eng. Struct.* 2024; 312: 118232.
  34. Guo Z., Zhang Y., Lu J., Fan J. Stiffness degradation-based damage model for RC members and structures using fiber-beam elements. *Earthq. Eng. Eng. Vib.* 2016; 15(4): 697–714.
  35. Han Q., Wang D., Zhang Y., Tao W., Zhu Y. Experimental investigation and simplified stiffness degradation model of precast concrete shear wall with steel connectors. *Eng. Struct.* 2020; 220: 110943.
  36. Li X., Liu J., Wang X., Dong B., Chen Y.F. Cyclic behavior of circular TSRC column to steel beam frames. *J. Constr. Steel Res.* 2021; 184: 106788.
  37. Yehia E., Khalil A.H., Mostafa E.-E., El-Nazzer M.A. Experimental and numerical investigation on punching behavior of ultra-high performance concrete flat slabs. *Ain Shams Eng. J.* 2023; 14(10): 102208.
  38. Abeer S.Z., Abdulridha S.Q., Nasr M.S., Hasan Z.A., Shubbar A. Improving the mechanical behavior of pervious concrete using polypropylene and waste rope fibers. *Al-Qadisiyah J. Eng. Sci.* 2024; 17(1): 38–46.
  39. Rashid M.A., Mansur M.A. Reinforced high-strength concrete beams in flexure. *ACI Struct. J.* 2005; 102(3): 462.
  40. Al-Ghamdy D.O., Wight J.K., Tons E. Flexural toughness of steel fiber reinforced concrete. *Eng. Sci.* 1994; 6(1).
  41. Shin S., Kang H., Ahn J., Kim D. Flexural capacity of singly reinforced beam with 150 MPa ultra high-strength concrete. 2010.
  42. Abbass A., Abid S., Özakça M. Experimental investigation on the effect of steel fibers on the flexural behavior and ductility of high-strength concrete hollow beams. *Adv. Civ. Eng.* 2019; 2019.
  43. Pam H.J., Kwan A.K.H., Islam M.S. Flexural strength and ductility of reinforced normal-and high-strength concrete beams. *Proc. Inst. Civ. Eng. Build.* 2001; 146(4): 381–389.
  44. Altoubat S., Yazdanbakhsh A., Rieder K.-A. Shear behavior of macro-synthetic fiber-reinforced concrete beams without stirrups. *ACI Mater. J.* 2009; 106(4).
  45. Altoubat S., Maalej M., Nassif N., Barakat S. Punching shear behavior of RC slabs incorporating macro-synthetic fibers. *J. Build. Eng.* 2023; 67: 105983.
  46. Wang Z., Yan J., Lin Y., Fan F. Punching shear performance of steel-fiber reinforced concrete-steel sandwich plates under different patch loading heads. *J. Build. Eng.* 2022; 48: 103955.
  47. Hassanli R., Youssf O., El-Naqeeb M.H., et al. Investigation of punching shear performance in concrete slabs reinforced with GFRP and synthetic fibers: An experimental study. *Eng. Struct.* 2024; 311: 118215.